

Contributions of Galectin-3 and -9 to Epithelial Cell Adhesion Analyzed by Single Cell Force Spectroscopy^{*[5]}

Received for publication, March 2, 2007, and in revised form, July 9, 2007. Published, JBC Papers in Press, August 3, 2007, DOI 10.1074/jbc.M701867200

Jens Friedrichs^{†1}, Juha M. Torkko^{§1}, Jonne Helenius[‡], Terhi P. Teräväinen[¶], Joachim Füllekrug^{||}, Daniel J. Müller[‡], Kai Simons[§], and Aki Manninen^{§¶2}

From the [§]Max Planck Institute of Molecular Cell Biology and Genetics, 01307 Dresden, Germany, the [†]Biotechnology Center, Dresden University of Technology, 01307 Dresden, Germany, the ^{||}Department of Internal Medicine IV (Gastroenterology), University of Heidelberg, 69120 Heidelberg, Germany, and [¶]Biocenter Oulu, Department of Medical Biochemistry and Molecular Biology, University of Oulu, P.O. Box 5000, FIN-90014 Oulu, Finland

Galectins are widely expressed in epithelial tissues and have been implicated in a variety of cellular processes, including adhesion and polarization. Here we studied the contributions of galectins in cell adhesion and cyst formation of Madin-Darby canine kidney cells. Quantitative single cell force spectroscopy and standard adhesion assays were employed to study both early (<2 min) and long term (90 min) adhesion of cells to different extracellular matrix components. Inhibitors were used to examine the contribution of integrins and galectins in general and RNA interference to specifically address the role of two abundantly expressed galectins, galectin-3 and -9. We found that both galectin-3 and -9 were required for optimal long term cell adhesion to both collagen I and laminin-111. Early adhesion to laminin was found to be integrin-independent and was instead mediated by carbohydrate interactions and galectin-3 and -9. The opposite was observed for early adhesion to collagen. Although similar, the contributions of galectin-3 and -9 to adhesion appeared to be by distinct processes. These defects in adhesion of the two galectin knockdown cell lines may underlie the epithelial phenotypes observed in the cyst assays. Our findings emphasize the complex regulation of epithelial cell functions by galectins.

Polarized epithelial cells are responsible for the integrity and function of the epithelial barrier (1, 2). Extracellular matrix (ECM),³ in particular the basement membrane, is not only

essential for structural support but also provides cues for epithelial differentiation and the orientation of apico-basal polarity (3, 4). Therefore, the characterization of interactions between ECM components and receptors at the cell surface is essential to understand the formation and maintenance of the epithelium.

Galectins constitute a family of structurally related proteins that bind to β -galactoside residues and interact with a broad spectrum of ligands (5, 6). Most if not all galectins are di- or multivalent and are therefore able to function as versatile cross-linkers of glycosylated cell surface molecules (7). Galectins have been shown to either promote or inhibit cell adhesion, depending on the galectin member studied as well as experimental condition (8). Galectins have also been implicated in the regulation of polarized membrane trafficking and cell-ECM interactions (9–12). Galectin-1 and galectin-3 null mice, as well as double-null mice, are viable and fertile but show subtle developmental and inflammatory phenotypes (13). In *Caenorhabditis elegans*, 3 of 26 predicted galectin-related genes have been associated with embryonic lethality or developmental abnormalities in large scale RNAi screens (5, 14, 15).

Here we studied the expression of several galectin family members in Madin-Darby canine kidney (MDCK) cells and used RNA interference (RNAi) to address the role of abundantly expressed galectin-3 and galectin-9 in cell adhesion and epithelial morphogenesis. A quantitative analysis of early events of cell-substratum adhesion was performed using single cell force spectroscopy (SCFS).

EXPERIMENTAL PROCEDURES

Cell Culture and Transfection—MDCK strain II cells were maintained in Earle's MEM (EMEM; PAA Laboratories) supplemented with 2 mM L-glutamine (Invitrogen), 100 units/ml penicillin, 100 μ g/ml streptomycin (Invitrogen) and with 5% FCS (PAA Laboratories; 10% for Transwell filter (Corning Costar) and cyst cultures). MDCK cells expressing the Myc-tagged galectin-9 were generated by retroviral transduction followed by hygromycin B (800 μ g/ml; BD Biosciences) selection for 3 days. The resulting cells were grown for up to 20 passages. The Phoenix gag-pol retroviral packaging cell line (obtained from the ATCC with authorization by Garry Nolan, School of Medicine, Stanford University, Stanford, CA) was kept in high glucose Dulbecco's modified Eagle's medium (Invitrogen) containing L-glutamine, penicillin/streptomycin, and 10% FCS.

* This work was supported by Deutsche Forschungsgemeinschaft Grant MU1791/3-2, European Commission Network Grant HPRN-CT-2002-00259, the Max-Planck-Society, and Academy of Finland Grant 114330. The costs of publication of this article were defrayed in part by the payment of page charges. This article must therefore be hereby marked "advertisement" in accordance with 18 U.S.C. Section 1734 solely to indicate this fact.

[5] The on-line version of this article (available at <http://www.jbc.org>) contains supplemental Table S1 and Figs. S1–S3.

¹ These two authors contributed equally to this work.

² To whom correspondence should be addressed: Biocenter Oulu, Dept. of Medical Biochemistry and Molecular Biology, University of Oulu, P.O. Box 5000, FIN-90014 Oulu, Finland. Tel.: 358-8-537-6081; Fax: 358-8-537-6115; E-mail: aki.manninen@oulu.fi.

³ The abbreviations used are: ECM, extracellular matrix; RNAi, RNA interference; MDCK, Madin-Darby canine kidney; SCFS, single cell force spectroscopy; EMEM, Earle's minimal essential medium; FCS, fetal calf serum; Gal3, galectin-3; Gal9, galectin-9; KD, knockdown; PBS, phosphate-buffered saline; DAPI, 4',6-diamidino-2-phenylindole; EST, expressed sequence tag; TRITC, tetramethylrhodamine isothiocyanate; AFM, atomic force microscopy; BSA, bovine serum albumin; Pcx, podocalyxin.

Functions of Galectin-3 and -9 in Epithelial Cells

For three-dimensional cell cultures, subconfluent MDCK cells were trypsinized and suspended to 5×10^6 cells/ml in PBS. Cells were pipetted into growth factor-reduced MatrigelTM (BD Biosciences) solution at 2×10^5 cells/ml and onto 24-well plates. After 30–45 min at 37 °C, medium was added, and the incubation was continued for 2–8 days. Medium was replaced every 2–3 days.

For transient transfections, 2×10^6 MDCK cells/condition were trypsinized, washed with PBS, and resuspended in 100 μ l of Nucleofector solution T (Amaxa Biosystems). DNA (4 μ g) was added, and electroporation was performed using program G-16 on an Amaxa Nucleofector (Amaxa Biosystems).

Antibodies and Constructs—The mouse monoclonal anti-Myc (9E10) antibody was provided by D. Drechsel (Max Planck Institute of Molecular Cell Biology and Genetics, Dresden, Germany). The gp135/podocalyxin antibody cell line, 3F2 (16, 17), was provided by G. Ojakian (State University of New York Downstate Medical Center, Brooklyn, NY) and A. M \ddot{u} sch (Cornell University, Ithaca, NY). Rat monoclonal integrin β -1 (AIIB2) antibody was provided by Karl Matlin (University of Chicago, Chicago, IL). Rat monoclonal galectin-3 (Mac-2; Cedarlane Laboratories Ltd.), RGD peptide (Sigma), mouse monoclonal integrin α -6 antibody (BD Biosciences), and fluorescein isothiocyanate- and Cy3-conjugated secondary antibodies (Jackson ImmunoResearch Europe Ltd.) were purchased.

Hamster galectin-3 cDNA was a gift of Dr. R. C. Hughes (National Institute for Medical Research, London, UK). Canine galectin-9 cDNA was PCR-amplified from our MDCK expressed sequence tag (EST) library. We obtained two variants (972 and 1068 bp; the latter, having a 96-bp insertion in its linker domain, was used). For the Gal9-6 \times Myc construct, an XbaI site was added between N-terminal lectin and linker domains. Six Myc tags were inserted into this site, and the Gal9-6 \times Myc fragment between BglII and XhoI restriction sites was subcloned into a BamHI/SalI-digested retroviral pBABE-hygro vector.

Retrovirus-mediated RNAi—Target sequences (Gal3-KD-528, GCT GAT AAC AAT TCT GGG CAC; Gal9-KD-298, GAG CTC TGC TTC ATG GTG AAC; Gal9-KD-867, GGA TGG TGA GCA CCT GTT TGA) corresponding to the canine galectin-3 (residues 528–548) and galectin-9 (residues 298–318 and 867–887) coding sequences were selected. Sequences were obtained from the MDCK EST library. Annealed oligonucleotides (supplemental Table S1) were cloned into an RVH-1-puro retroviral vector, and recombinant knockdown (KD) viruses were generated as described previously (18). Subconfluent MDCK strain II cells were trypsinized, and 5×10^5 cells in 3 ml of complete EMEM (5% FCS) supplemented with 4 μ g/ml of hexadimethrine bromide (Polybrene; Sigma) were seeded onto a 3.5-cm diameter culture dish (Corning Costar). The following day, medium was aspirated, and 1 ml of virus-containing pre-cleared supernatant from Phoenix cells was added. Hexadimethrine bromide (4 μ g/ml) was added to virus preparations. One hour later, 1 ml of fresh complete EMEM (5% FCS) was added, and the incubation was continued for 8–12 h. Infection was repeated 1–2 times before cells were trypsinized and reseeded in EMEM containing 4 μ g/ml puromycin (BD Bio-

sciences). Maximum knockdown efficiencies were obtained after 2–3 days of puromycin selection, and the KD cells were used for up to 2 weeks without a significant drop in knockdown efficiency. Knockdown efficiency was analyzed by RT-PCR as described previously (18) (Table S1).

Immunofluorescence—For surface labeling, filter-grown (4 days) MDCK cells were washed twice with ice-cold serum-free EMEM and subsequently kept on ice to prevent endocytosis. Filters were incubated for 45 min in serum-free medium containing β 1-integrin (AIIB2; 1:10) or α 6-integrin (1:100) antibodies on both apical and basolateral sides. Cells were washed twice with EMEM and twice with PBS containing 0.9 mM Ca²⁺ and 0.5 mM Mg²⁺ (PBS⁺), followed by MeOH fixation. For intracellular and extracellular staining of integrins, cells on filters were washed once with PBS and fixed with MeOH prior to the addition of primary antibodies. Filters were cut out of their supports and washed in PBS⁻. Nonspecific binding was blocked in PBS⁻ containing 0.1% fish skin gelatin (Sigma) and 0.5% BSA (Sigma) for 30 min. Filter pieces were incubated with secondary antibodies (1:500 in blocking solution) containing DAPI (0.6 μ M; Sigma) for 45 min, washed extensively in PBS⁻, and mounted onto slides with MowiolTM.

MDCK cysts in three-dimensional gels were washed with PBS⁺ and incubated for 20 min in PBS containing 4% paraformaldehyde (PFA; Sigma). After a PBS wash, residual aldehyde was quenched for 20 min in PBS⁻ containing 200 mM glycine (Sigma). Cells were permeabilized for 20 min in PBS⁻ with 0.1% Triton X-100 (Sigma), incubated in blocking solution for 30 min. Primary antibodies (1:200 anti-Myc and anti-Pcx, 1:400 anti-galectin-3; dilutions in blocking solution) were added and incubated overnight at 4 °C, washed extensively in PBS followed by overnight incubation at 4 °C with 1:500 dilutions of fluorophore-conjugated secondary antibodies. When indicated, DAPI and TRITC-phalloidin (0.1 μ M; Sigma) were added with the secondary antibodies. Gels were washed in PBS, removed from the plates, and mounted onto slides with MowiolTM. Images were acquired with an OLYMPUS FluoView-1000 (Olympus; using a 60 \times PlanApo oil objective, numerical aperture 1.1) laser-scanning confocal microscope.

Galectin-9 Secretion—MDCK-Gal9myc cells grown for 3–4 days on 12-mm Transwell filters were washed twice with starvation medium (EMEM lacking methionine and cysteine (PAA Laboratories), containing L-glutamine and antibiotics) before a 15-min incubation in starvation medium at 37 °C. Cells were labeled by placing the filter onto a 20- μ l drop of labeling medium (starvation medium containing 30 μ Ci of [³⁵S]methionine) for 20 min. Filters were washed twice with chase medium (complete EMEM containing 5% FCS and 150 μ g/ml unlabeled methionine) prior to incubation in chase medium at 37 °C. Apical and basolateral medium and cells were harvested at the indicated times. Galectin-9 was immunoprecipitated using an anti-Myc antibody (9E10) and Protein G-Sepharose beads (Sigma). Precipitated proteins were separated and visualized by SDS-PAGE and autoradiography.

Standard Cell Adhesion Assay—Cell adhesion was determined as described previously (19). Briefly, subconfluent MDCK cells were detached in PBS⁻ containing 2 mM EDTA and 0.5 mM EGTA at 37 °C. Cells were pelleted and resus-

pended in serum-free medium at 2×10^6 cells/ml. Fifty microliters of cell suspension was pipetted into 96-well plate wells coated with laminin-111 (20) (20 $\mu\text{g/ml}$; Sigma), collagen I (3 $\mu\text{g/ml}$; Nutacon), MatrigelTM (40 $\mu\text{g/ml}$), BSA (1%; Sigma), or poly-D-lysine (100 $\mu\text{g/ml}$; Sigma) containing 50 μl of 1% BSA in serum-free medium. When indicated, cells were resuspended and incubated in ice-cold serum-free medium containing 50 mM D-lactose (Sigma), 100 $\mu\text{g/ml}$ RGD peptide (Sigma), or a 1:10 dilution of AIIB2 for 30 min prior to plating. Plates were incubated at 37 °C for 90 min followed by four washes with PBS⁺ to remove nonadherent cells. Adherent cells were fixed in methanol, stained with crystal violet (0.1% w/v; Sigma), lysed in 10 mM HEPES, pH 7.4, containing 1% (w/v) sodium deoxycholate, and quantified using a spectrophotometer (absorbance at 540 nm from which the background at 405 nm was subtracted).

Single Cell Force Spectroscopy Instrumentation—Force spectroscopy was conducted using a NanoWizard (JPK Instruments), mounted on a Zeiss Axiovert 200 M microscope (Carl Zeiss). The NanoWizard atomic force microscope (AFM) was equipped with the CellHesion module (JPK Instruments) that extended the vertical movement range to 100 μm . A BioCell stage incubator (JPK Instruments) allowed measurements to be conducted at 37 °C. Cantilevers used were 200- μm -long V-shaped silicon nitride tipless cantilevers with nominal spring constants of 0.06 N/m (NP-0, Veeco). Cantilever spring constants were calibrated prior to use by routines included in the AFM software (21).

Surface Coating of AFM Cantilever and Coverslips—Cantilevers were cleaned in 2% Hellmanex (Hellma GmbH), residual air plasma-cleaned for 1 min and incubated at 4 °C in 2 mg/ml concanavalin A (from *Canavalia ensiformis*; Sigma) in PBS overnight. Before use, cantilevers were extensively washed in PBS.

Glass coverslips ($\varnothing 24$ mm) were cleaned by sequential washes in 1M HCl, water, and EtOH and air-dried. Thereafter, coverslips were incubated with 5 $\mu\text{g/ml}$ laminin-111 in PBS for 2 h at 37 °C. For collagen coating, mica discs ($\varnothing 6.5$ mm) were glued (OP-29; Dymax Europe GmbH) onto the center of glass coverslips ($\varnothing 24$ mm). Then solubilized bovine dermal collagen (3 mg/ml; Cohesion) was diluted to 30 $\mu\text{g/ml}$ in coating buffer (200 mM KCl, 50 mM glycine, pH 9.2) and was then added to the freshly cleaved mica discs and incubated overnight at room temperature (22). Prior to use, unbound protein was removed by washing, first with PBS then with fresh measurement medium (see below).

Cell Capture, Force Measurement, and Data Processing—Approximately 12 h prior to adhesion experiments, the MDCK cell growth medium was replaced by CO₂-independent medium (Invitrogen) supplemented with L-glutamine, penicillin/streptomycin, and 1% FCS. Prior to measurements, cells were washed once with PBS⁻, trypsinized, pelleted, and resuspended into serum-free CO₂-independent medium (measurement medium) and allowed to recover for 15 min. When indicated, medium was supplemented with 50 mM lactose or 5 mM EDTA. Integrin-blocking antibodies (1:10 dilution of the hybridoma supernatant) and RGD peptides (100 $\mu\text{g/ml}$) were incubated together with cells on ice for 30 min prior to analysis.

Functions of Galectin-3 and -9 in Epithelial Cells

Thereafter, cell suspensions were pipetted into the BioCell containing a coated coverslip and allowed to settle for 5 min. The apex of a calibrated concanavalin A-coated cantilever was positioned above a cell before it was lowered (speed, 5 $\mu\text{m/s}$) until an absolute force of 0.75 nN was applied to the cells. After 5 s, the cantilever-bound cells were retracted (50 μm) and allowed to adhere for at least 5 min. For force curve measurements, the approach and retract rates were set to 5 $\mu\text{m/s}$, and the contact force was set to 0.75 nN. Depending on the contact time (2–90 s), the pulling range was adjusted between 15 and 60 μm . For short contact times (2–20 s), 5–10 force curves were recorded with resting periods of 10 s between approach/retract cycles. Cells were allowed to recover for ~5 min, before a new set of force curves was acquired. A maximum of 30 curves were acquired per cell. At 90 s contact time, force curves were recorded at 3-min intervals, never exceeding five force curves per cell. Loss of adhesion strength with force curve cycle was not observed.

Detachment forces and step size and step number were extracted using in-house algorithms in Igor Pro 5.04 (WaveMetrics). InStat3 (GraphPad) was used to perform statistical tests on data sets.

RESULTS

Expression of Galectins in MDCK Cells—The relative expression levels of selected galectins, known to be expressed in the kidney (galectins 1, 3, 8, and 9) and/or containing tandem carbohydrate recognition domains (galectins 4, 6, 8, 9, and 12), were analyzed using quantitative real time PCR (Fig. 1A). Galectin-3 was expressed at very high levels. Galectin-9, -8, and -1 were relatively abundant, whereas only low levels of galectin-6 and -12 mRNAs were found. Galectin-4 mRNA was not detected. Hereafter, we limited our studies to galectin-3 and -9, the two most abundantly expressed galectins.

Retroviral RNAi was employed to specifically and efficiently inhibit (>90%) the expression levels of galectin-3 or -9 mRNAs (Fig. 1B) (18). MDCK cells infected with retroviruses lacking a target sequence in their short hairpin RNA expression cassette were used as a control in all experiments. Protein levels in galectin-3 knockdown (Gal3-KD) and Gal9-KD cells were analyzed by Western blotting. Endogenous galectin-3 was detected using galectin-3 antibodies. Due to the lack of a suitable antibody against canine galectin-9, MDCK cells expressing Myc epitope-tagged canine galectin-9 (MDCK-Gal9myc) were generated by retroviral transduction. The efficiency of the Gal9-KD construct at protein level was analyzed in MDCK-Gal9myc cells using antibodies against the Myc epitope. The observed reduction (~90%) in galectin-3 and -9 protein levels in KD cells correlated well with the reduction seen in mRNA levels (Fig. 1B).

Galectin-3 and -9 Contribute to Cell Adhesion—To assess the role of the two galectins in epithelial long term adhesion, tissue culture plates were coated with laminin-111, the major component of the basement membranes; MatrigelTM (23), a solubilized basement membrane-like matrix; or collagen I. Single cell suspensions were seeded onto the coated plates and allowed to adhere for 90 min before nonadhering cells were washed off. When integrin-mediated adhesion was blocked by chelating free calcium and magnesium, cells did not adhere to any of the

Functions of Galectin-3 and -9 in Epithelial Cells

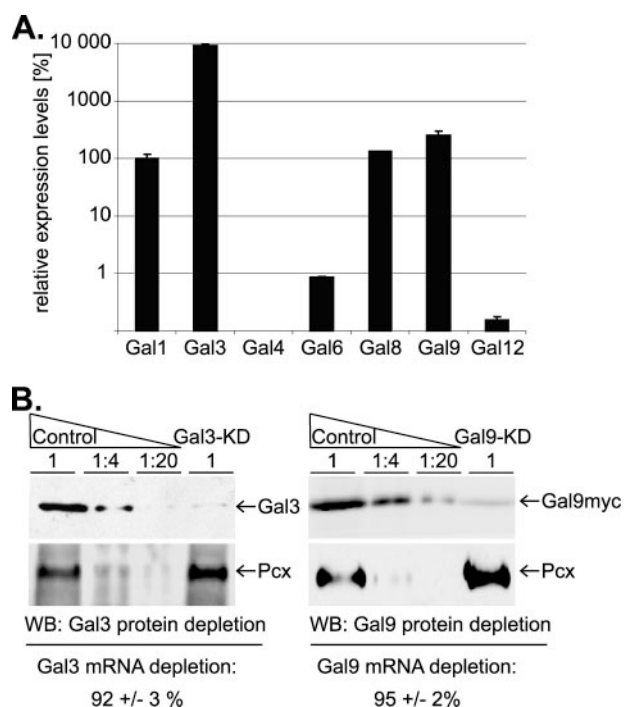


FIGURE 1. Expression of galectins in MDCK cells. *A*, mRNA expression levels of seven galectin family members in MDCK cells were analyzed using real-time PCR. Galectin-1 mRNA level was set to 100%, and expression of the other galectin mRNAs relative to this are plotted ($n = 3$). Error bars denote S.D. unless stated otherwise. *B*, galectin-3 and -9 levels in control and KD cells were determined by Western blot (WB) and real time PCR analysis. Lysates from puromycin-selected MDCK cells infected with control or Gal3-KD viruses (*left*) and MDCK-Gal9myc cells infected with control or Gal9-KD viruses (*right*) were assayed for expression of endogenous galectin-3 or ectopically expressed Gal9myc using galectin-3 or Myc antibodies, respectively. Dilutions of the control cell lysates (1 = 20 μ g of total protein, 1/4 = 5 μ g, and 1/20 = 1 μ g) were loaded to allow residual galectin protein levels in the KD cells (20 μ g of total protein loaded) to be estimated. Podocalyxin was used as a loading control.

coatings, demonstrating the involvement of integrins in cell adhesion in this assay (data not shown). Preincubation of cells with competitive inhibitors of galectin sugar-binding activity, D-lactose or galactose, slightly reduced the adhesion, suggesting that carbohydrate-dependent interactions may play a role (Fig. 2A). The contribution of integrins was more specifically confirmed using function-blocking β 1-integrin antibodies (AIIB2) and competitive inhibitory RGD peptides. Although β 1-integrins were found to be essential for adhesion to all of the matrices studied, RGD peptide, an inhibitor of integrin receptors for fibronectin matrix (19), did not affect adhesion (Fig. 2A). The specific roles of galectin-3 and -9 were addressed by studying the adhesion of galectin-depleted cells. Compared with control cells, both Gal3- and Gal9-KD cells adhered less efficiently to laminin-111, collagen I (Fig. 2B), and MatrigelTM (Fig. S1).

The possibility of RNAi off target effects (24) was examined. To this end, galectin-3 expression was rescued by transiently transfecting Gal3-KD cells with a hamster galectin-3-encoding expression vector. This galectin-3 ortholog differs from the canine galectin-3 at the RNAi target region, making it resistant to silencing by the short hairpin RNA with the canine sequence. Hamster galectin-3 expression in Gal3-KD MDCK cells led to a robust increase in adhesion, indicating that the observed adhe-

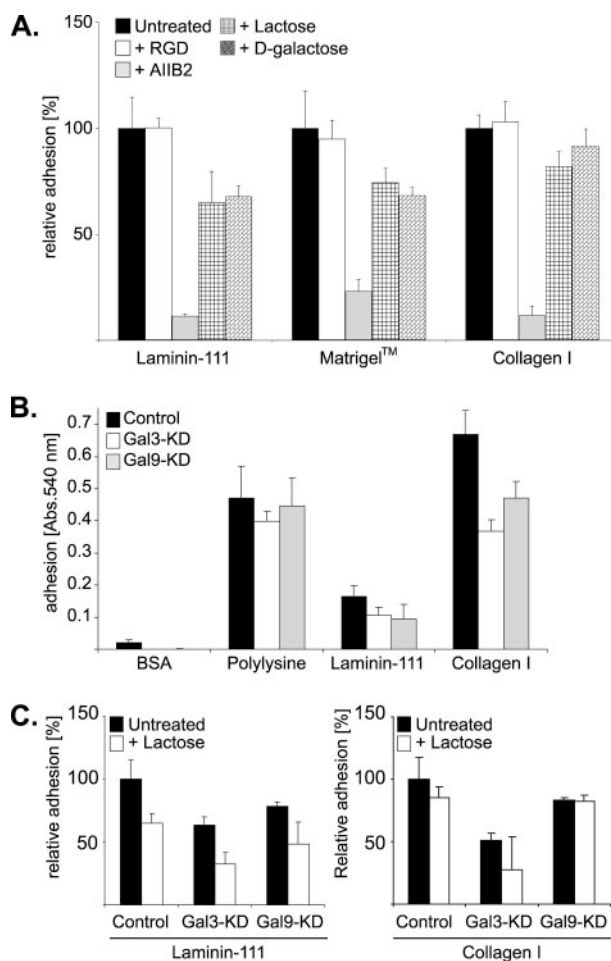


FIGURE 2. Galectin-3 and galectin-9 contribute to cellular adhesion. *A*, single cell suspensions of MDCK cells were allowed to settle for 90 min on laminin-111-, MatrigelTM-, or collagen I-coated tissue culture wells. When indicated, cell suspensions were incubated for 30 min on ice in medium supplemented with 50 mM D-lactose, 50 mM D-galactose, a 1:10 dilution of β 1-integrin function blocking antibody, or 100 μ g/ml RGD-peptide prior to plating. Nonadherent cells were washed away, and remaining adherent cells were fixed, stained, and quantified ($n = 3$). Adhesion of untreated cells to each coating was set to 100%, and adhesion of treated cells is shown relative to this. *B*, adhesion of control, Gal3-KD, and Gal9-KD MDCK cells on BSA-, poly-D-lysine-, laminin-111-, or collagen I-coated plates was assayed as described in *A* ($n = 5$). BSA and poly-D-lysine coatings served as a negative and positive control, respectively. *C*, adhesion of control, Gal3-KD, and Gal9-KD cells to laminin-111 (*left*) and collagen I (*right*) in the absence and the presence of 50 mM lactose ($n = 3$).

sion defect in Gal3-KD cells was specifically due to lack of galectin-3 expression (Fig. S1A). With galectin-9, we used an alternative approach to confirm the specificity. A second target sequence (nucleotides 867–887) for canine galectin-9 from a different region of the galectin-9 mRNA was selected. This retroviral Gal9-KD2-construct resulted in efficient depletion of galectin-9 mRNA ($90 \pm 3\%$ as measured by quantitative real time PCR) and protein levels (data not shown) in MDCK cells. Furthermore, we found that adhesion to MatrigelTM was reduced to a similar extent in both Gal9-KD cell populations (Fig. S1B). The probability that the two distinct RNAi targets in the galectin-9 sequence would lead to same off-target effects is negligible. Thus, we concluded that the effects of galectin-3 and -9 depletion on adhesion were specific.

Interestingly, the already reduced adhesion of cells by 50 mM lactose was further reduced in Gal3- and Gal9-KD cells (Fig. 2C). This suggests that the galectins have functions that are not mediated by their sugar-binding domain at the cell surface. These could be indirect mechanisms, such as regulating integrin function or localization. In conclusion, the long term stable adhesion to laminin and collagen was β 1-integrin-dependent, but both galectin-3 and -9 were required for maximal adhesion efficiency.

To get a more quantitative insight into the early cell-substrate adhesion events, SCFS was applied (25) (Fig. S2). In this approach, single cells were attached to a concavalin A-coated AFM cantilever and lowered onto laminin-111- or collagen I-coated substrates. Upon retraction, the maximum detachment force was determined. Surprisingly, in contrast to long term cell adhesion, early adhesion to laminin-111 was found to be integrin-independent, since chelation of divalent ions by EDTA or the addition of β 1-integrin function blocking antibodies had no significant effect (Fig. 3, B and C). Instead, carbohydrate-mediated interactions were important, as evidenced by the ability of lactose to inhibit cell adhesion to laminin-111 (Fig. 3B). The opposite was observed for early adhesion to collagen I, which was found to be entirely dependent on functional β 1-integrin (Fig. 4, B and C). In both cases, RGD-binding integrins were dispensable for adhesion (Figs. 3C and 4C). In agreement with lactose insensitivity, adhesion to collagen I was not affected in Gal3- and Gal9-KD cells (Fig. 4A). On the contrary, a clear reduction was evident in the adhesion to laminin-111 of Gal3- and Gal9-KD cells, compared with control cells, suggesting that galectins, via their sugar-binding domains, play an important role in the early adhesion to laminin-111 (Fig. 3A).

To exclude the possibility that galectin depletion resulted in cytoskeletal or morphological changes that influenced cell adhesion measurements, cell elasticity was studied (26). Significant differences were not found between cells, confirming that the decrease in the maximum detachment force was not due to gross differences in KD cell elasticity or size but instead represented a difference in adhesion between cells and substratum (data not shown).

Cell detachment did not occur via a single rupture event but via a number of smaller steps of varying size representing the disruption of single adhesion units or clusters (Fig. S2). The sizes as well as the average number of such individual steps within force curves recorded after 90 s contact time to laminin-111 were analyzed (Fig. 5). Although the relatively small number of curves analyzed (control, $n = 82$; Gal3-KD, $n = 35$; Gal9-KD, $n = 48$) only allows statistical significance to be assigned to the difference in rupture steps per curve, an interesting trend was observed. Compared with control cells, Gal9-KD cells had slightly smaller steps (Fig. 5A), whereas Gal3-KD cells had fewer steps per curve (Fig. 5B). This suggested that the mechanism by which these two galectins affect cell adhesion to laminin-111 is different. It is tempting to speculate that whereas galectin-9 mainly contributed directly to the adhesion, galectin-3 affected the number of adhesive interactions.

Comparative analysis of the step sizes in the force curves recorded in control cells after 90-s contact with collagen I (inte-

Functions of Galectin-3 and -9 in Epithelial Cells

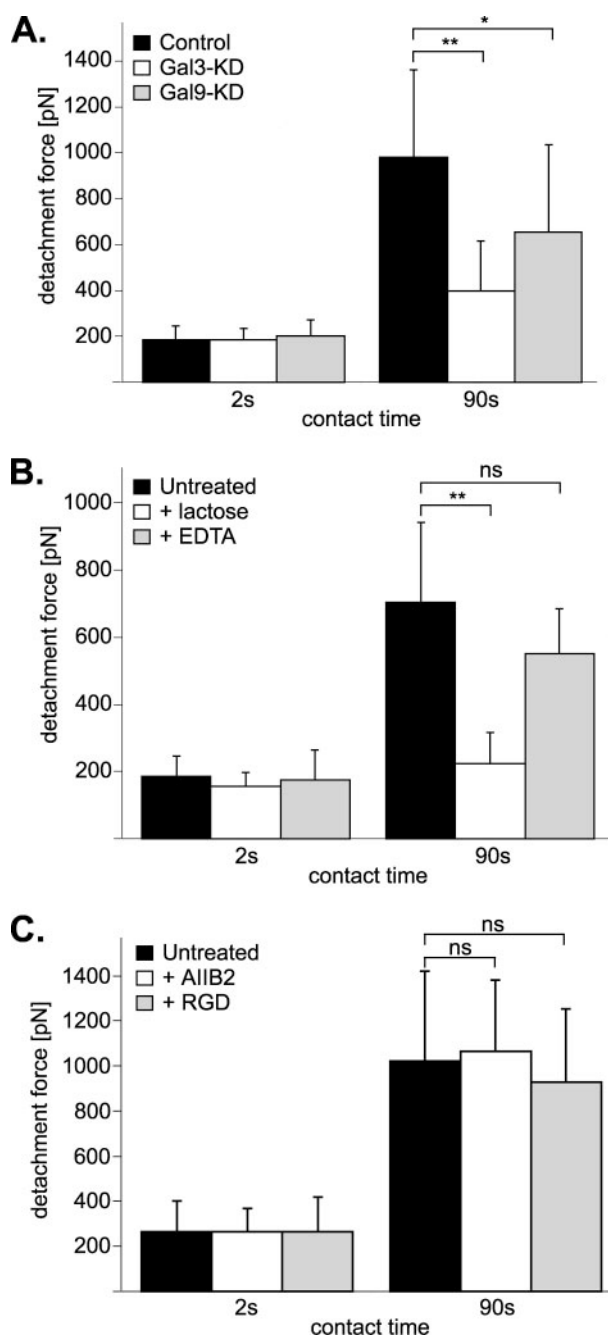


FIGURE 3. SCFS analysis of adhesion to laminin-111. A, single control (2 s, $n = 53$; 90 s, $n = 21$), Gal3-KD (2 s, $n = 24$; 90 s, $n = 23$), or Gal9-KD (2 s, $n = 26$; 90 s, $n = 20$) MDCK cells were captured onto concavalin A-coated AFM cantilevers and pressed onto laminin-111-coated substrates. After the indicated contact times, cells were lifted from the substrate, and the maximum detachment force was recorded as described under "Experimental Procedures." ns, no significance ($p > 0.05$); *, $p < 0.05$; **, $p < 0.001$. B, the maximum detachment force between MDCK cells and laminin-111 was measured in the absence and presence of 50 mM lactose or 5 mM EDTA. At least 20 cells were analyzed for each condition. C, the maximum detachment force between MDCK cells and laminin-111 was measured in the absence and presence of β 1-integrin function blocking antibody (AIB2; diluted 1:10) or 100 μ g/ml RGD peptide. At least 15 cells were analyzed for each condition.

grin-mediated) and laminin-111 (galectin-mediated) showed a significant difference between these two types of interactions. Integrin-mediated interactions with collagen I were generally stronger (the most probable force 86.42 pN; Fig. 5C) than galectin-mediated interactions to laminin-111

Functions of Galectin-3 and -9 in Epithelial Cells

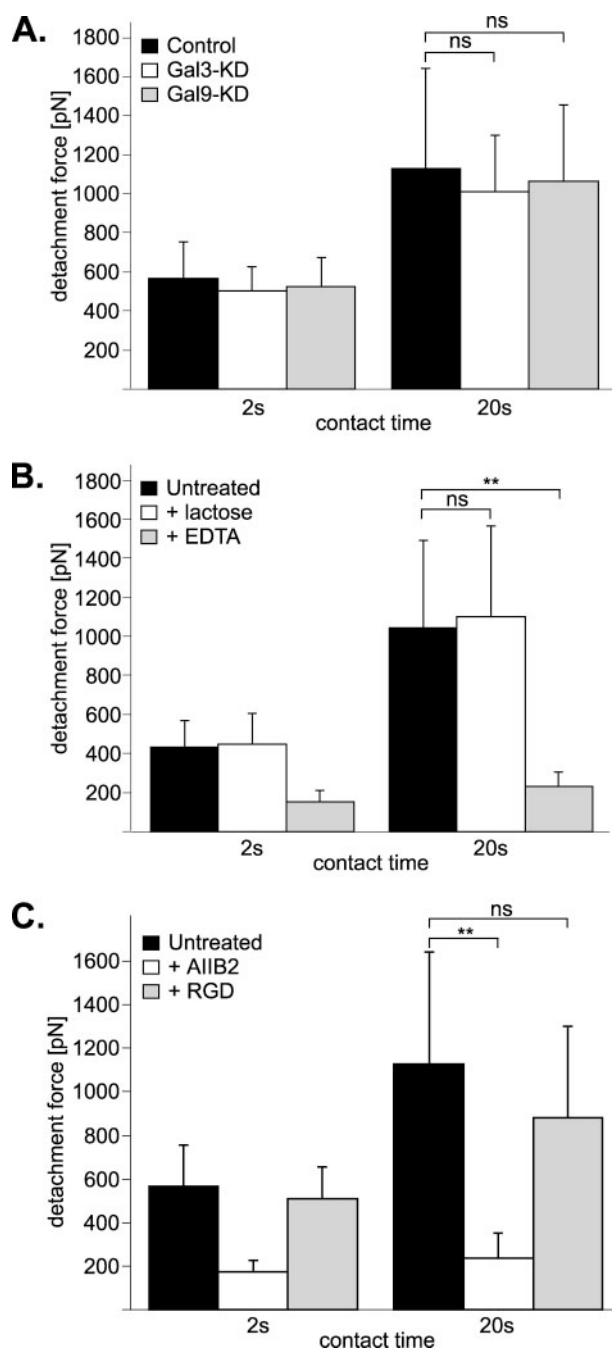


FIGURE 4. SCFS analysis of adhesion to collagen I. *A*, single control (2 s, $n = 21$; 20 s, $n = 20$), Gal3-KD (2 s, $n = 20$; 20 s, $n = 19$), or Gal9-KD (2 s, $n = 22$; 20 s, $n = 21$) MDCK cells were captured onto concavalin A-coated AFM cantilevers and pressed onto collagen I-coated substrates. The maximum detachment force was recorded. *ns*, $p > 0.05$; *, $p < 0.05$; **, $p < 0.001$. *B*, the maximum detachment force between MDCK cells and collagen I was measured in the absence and presence of 50 mM lactose or 5 mM EDTA. At least 15 cells were analyzed for each condition. *C*, the maximum detachment force between MDCK cells and collagen I was measured in the absence and presence of $\beta 1$ -integrin function-blocking antibody (AIB2; diluted 1:10) or 100 $\mu\text{g}/\text{ml}$ RGD peptide. At least 15 cells were analyzed for each condition.

(60.02 pN), further supporting the conclusion that different kinds of machineries are involved in early adhesion processes to these two matrices.

Surface Expression of Major ECM Receptor Integrins Is Normal in Galectin-3- and Galectin-9-depleted MDCK Cells—In addition to the direct role of galectins in early laminin-111

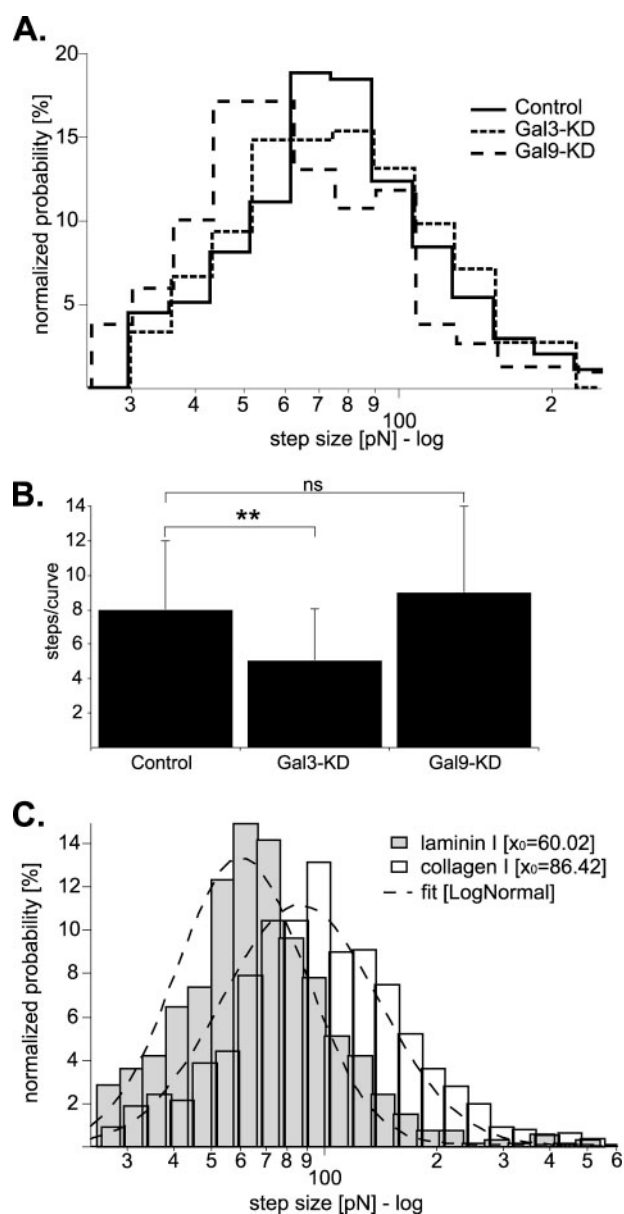


FIGURE 5. Analysis of the small detachment steps in force curves recorded after 90 s of cell-substrate contact. *A*, the distribution of the step sizes for control, Gal3-KD, and Gal9-KD MDCK cells in force curves recorded after 90-s contact with laminin-111 was determined and plotted according to the normalized step size probability. *B*, the average number of steps per force curve (90-s contact times) in control, Gal3-KD, and Gal9-KD MDCK cells was determined. *ns*, $p > 0.05$; **, $p < 0.001$. *C*, the distribution of the step sizes in retraction force curves recorded after control cells had been in contact with laminin-111 (galectin-mediated, gray bars) and collagen I (integrin-mediated, white bars) for 90 s.

adhesion, galectins were also found to regulate stable integrin-dependent adhesion via an indirect mechanism (Fig. 2*B*). Galectin-3 has been shown to regulate the subcellular localization of $\beta 1$ -integrins (27). To test if altered localization of ECM receptors may explain the observed adhesion defects, we analyzed the surface expression of the major integrin receptors in galectin-depleted MDCK cells. Polarized filter-grown cells were chilled on ice to prevent endocytosis, and cell surfaces (both apical and basolateral) were probed using $\beta 1$ - or $\alpha 6$ -integrin antibodies. A strong lateral signal and less intense basal staining were detected with $\beta 1$ -integrin anti-

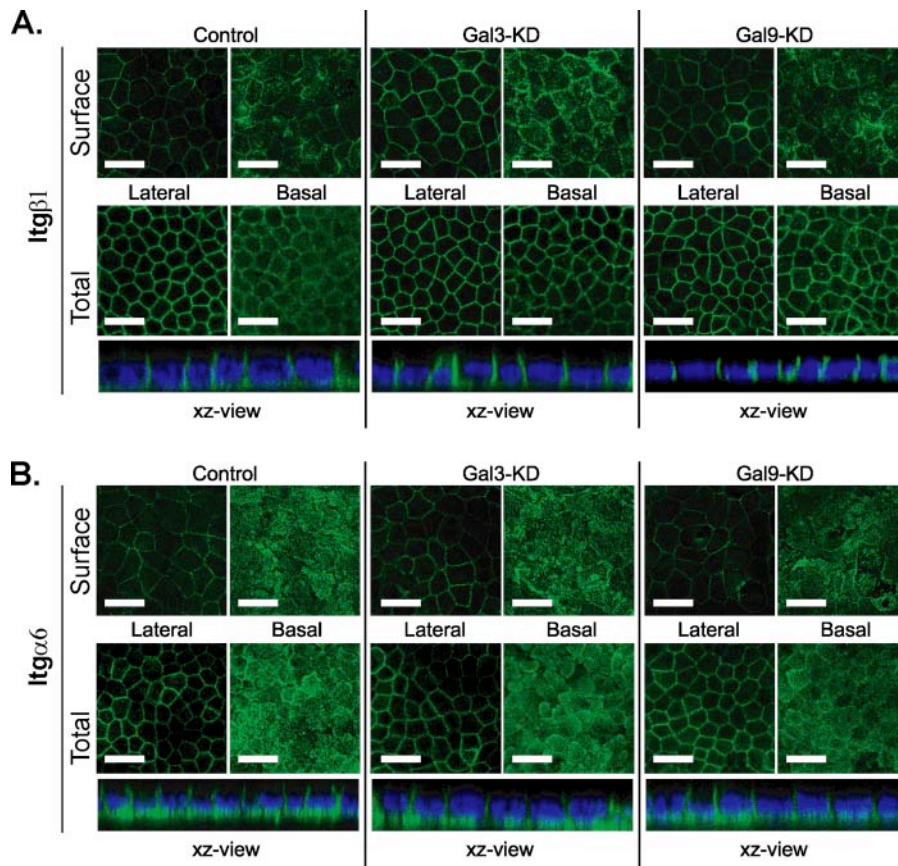


FIGURE 6. Subcellular localization of integrins in control, Gal3-KD, and Gal9-KD MDCK cells. To reveal integrins exposed at the apical and basolateral surfaces, control, Gal3-KD, and Gal9-KD MDCK cells were grown on Transwell filters (4 days), transferred on ice to block endocytosis, and incubated for 45 min with $\beta 1$ -integrin (green, upper panels in A) or $\alpha 6$ -integrin (green, upper panels in B) antibodies. After incubation, filters were washed, fixed, and processed for immunofluorescence. Nuclei were stained with DAPI (blue). For total integrin staining, filter-grown (4 days) control, Gal3-KD, and Gal9-KD MDCK cells were fixed and permeabilized with MeOH and stained using $\beta 1$ -integrin (A) or $\alpha 6$ -integrin (B) antibodies (lower panels including an xz view). Stacks from the middle (Lateral) and the basal level (Basal) are shown. Scale bars, 20 μ m.

bodies (Fig. 6A). $\alpha 6$ -Integrin antibodies showed a robust basal signal and fainter staining at the lateral membranes (Fig. 6B). When permeabilized cells were stained for these integrins only, some intracellular vesicular structures were seen, indicating that, at steady state, the majority of integrins are at or close to the cell surface. No significant differences could be found between the control and galectin-depleted cells, suggesting that subcellular distribution and surface expression of the major integrin receptors were not affected by the absence of galectin-3 or -9.

Cystogenesis of Galectin-3 and -9-depleted MDCK Cells—Adhesive cell-ECM interactions are thought to regulate epithelial morphogenesis. When cultured in three-dimensional proteinaceous gel matrices, MDCK cells form polarized multicellular cysts. Cyst cultures are frequently used to reveal subtle defects in epithelial morphogenesis (28). Control, Gal3-KD, and Gal9-KD cells were seeded into MatrigelTM, and the progression of cystogenesis was followed by collecting samples at days 2, 4, and 8. In these culture conditions, parental MDCK cells form hollow spherical cysts with dilated lumens within 4–5 days. Compared with control cells, cystogenesis of both galectin-KD cell types was delayed (Fig. 7A). Although the majority of control cysts had formed smooth-surfaced, dilated

lumens by the fourth day in culture, most of the Gal3-KD cysts and almost half of the Gal9-KD cysts still had small lumens with irregular surfaces (Fig. 7A). Because cystogenesis requires cell division, the growth kinetics of control and KD cells was assayed by counting them over a period of 1 week. Although Gal9-KD cells grew at the same rate as control cells, Gal3-KD cells grew slower (Fig. 7B), indicating that the delay in Gal3-KD cell cystogenesis might be in part due to decreased growth rate. Cell polarity in developing cysts was studied by following an early apical membrane marker, podocalyxin (Pcx) (16). Although unpolarized surface expression of Pcx was frequently observed in developing Gal3-KD cysts (>60% at day 2, examples shown in the left column in Fig. 7A), significant mistargeting was not observed in Gal9-KD cells (15% at day 2) compared with controls (10% at day 2). When analyzed at day 8, the majority of both Gal3- and Gal9-KD cysts had fully matured, and their surface polarity and overall morphology was similar to that of control cysts (Fig. 7A; data not shown). In conclusion, the cyst analysis demonstrated that both Gal3-KD and Gal9-KD cells exhibited delayed cystogenesis.

The surface polarity of KD cells was either transiently (Gal3) or not (Gal9) affected.

DISCUSSION

Our data show that both galectin-3 and -9 are involved in cell-matrix interactions. Adhesion is a dynamic process where initial contacts are mediated by limited number of interacting molecules. The early interactions regulate a complex process of recruitment and clustering of additional components, leading to formation of organized adhesion complexes and focal adhesions. This is highlighted by findings that the adhesion strength at the single cell level does not uniformly and gradually increase with contact time but shows complex behavior and cell-to-cell variation at contact times exceeding 2 min (29). Due to the small molecular forces involved, studying the early adhesion phase poses a methodological challenge.

This is the first study of epithelial cell adhesion using SCFS. We show that this quantitative method can be combined with RNAi to study the role of specific genes in cellular adhesion. SCFS measures early aspects of adhesion different from a traditional gravitational assay, where cells typically have more than 1 h to interact with the substratum. This kinetic aspect opens up new questions concerning functional and molecular

Functions of Galectin-3 and -9 in Epithelial Cells

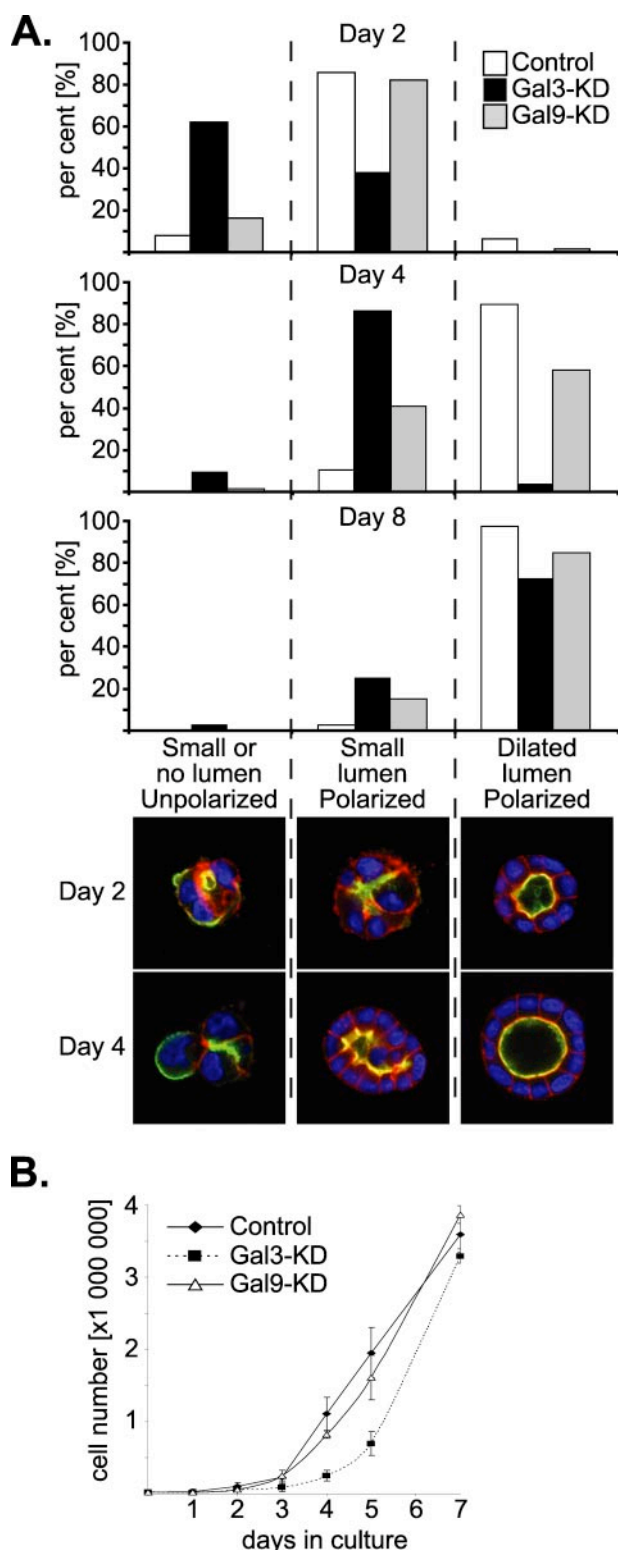


FIGURE 7. Galectin-3 and galectin-9 are required for efficient cystogenesis in MDCK cells. A, control, Gal3-KD, and Gal9-KD MDCK cells were grown in Matrigel™ for 2, 4, and 8 days. Developing and mature cysts were stained for DNA (DAPI; blue), filamentous actin (TRITC-phalloidin; red), and podocalyxin (Pcx antibodies; green). Labeled cysts were phenotypically classified into three categories, unpolarized (Pcx staining seen also at the basolateral membrane), small apical lumen (polarized immature cyst), and dilated apical lumen (polarized mature cyst). The data are representative of three independent experiments. 60–100 control or KD cysts were analyzed for each time point in the experiment shown. B, 20,000 control, Gal3-KD, and Gal9-KD MDCK cells were seeded onto tissue culture dishes (03.5 cm). Cells were counted on days 1, 2, 3, 4, 5, and 7.

links between early and late phases of adhesion. Although galectins seem to have a supportive role in the formation of integrin-mediated strong adhesion to laminin-111, our data show that initial contacts are mainly carbohydrate-mediated and largely depend on galectins. In contrast, early adhesion to collagen I is galectin-independent and mediated solely by integrins. However, the long term adhesion to collagen I again seems to be strengthened by galectins. It appears that galectins regulate adhesion at multiple levels.

Given the carbohydrate-binding abilities of galectins, it is probable that they modulate adhesion from the extracellular side. Although lacking signal sequences, some galectins, including galectin-3, are secreted from cells via a nonclassical pathway (30–32). We found that galectin-9 was likewise secreted from MDCK cells (Fig. S3A). Thus, galectin-3 and -9, being multivalent, might directly form cell-ECM interactions. Alternatively, their function in adhesion is indirect. To this end, galectins have been implicated in the regulation of integrin activation and/or trafficking (27, 33–35). Although no obvious alterations of the steady state surface expression of the major integrins were observed in galectin-depleted cells, the data do not exclude more subtle, dynamic changes in integrin trafficking or activity. More detailed studies are necessary to conclusively address this issue.

The link between cell adhesion and epithelial morphogenesis is of great importance. It has been concluded that in cyst cultures, efficient secretion takes place at the basal side (36). In cyst cultures, cytoplasmic galectin-3 accumulates in the subbasal region that faces the ECM (9). We found that galectin-9 behaves similarly (Fig. S3B). The secretion and subbasal localization of galectin-3 and -9 are in agreement with a role in regulated adhesive interactions. In the study by Bao and Hughes (9), the addition of recombinant galectin-3 retarded cyst expansion, whereas inhibition of galectin-3 function by antibodies enhanced the growth of cells. Interestingly, the same approach yielded similar conclusions for the growth-inhibitory role of galectin-3 in ureteric branching tubulogenesis in mouse kidney explants (37). It was proposed that secreted galectin-3 restricts the growth and expansion of epithelium by stabilizing and/or modulating basal interactions between cells and the ECM (9). Contrary to the positive effect on growth of the galectin antibodies, we observed reduced proliferation of Gal3-KD cells. Although the different methods of galectin-3 inhibition (antibody blocking only extracellular galectin functions *versus* RNAi depleting galectin expression in cells) most likely underlie the differing results, it is possible that the proliferation defect in Gal3-KD cells is mechanistically distinct from the proposed role of galectin-3 at the cyst surface. Because the time frame required for the cyst expansion assay (clear differences observed only after 12–20 days) is well beyond the time frame of our experimental setup (up to 8 days), the data do not exclude the latter.

Adequate assembly of the basal laminin networks is required for proper MDCK cystogenesis (38). Assembly requires not only homo- and hetero-oligomeric interactions between laminin and other ECM molecules but also concentration of laminin at the cell surface and anchoring of the basal membrane to the nascent networks. Galectins are possibly involved in the assem-

bly of laminin and other ECM networks. Such a function was described by Al-Awqati and co-workers (10) when they showed that galectin-3 was necessary for polymerization of hensin, which in turn induced terminal differentiation of the epithelia. Since galectin-3 binds laminin, a similar induced laminin assembly mechanism could be envisioned (39). Perturbed laminin assembly could underlie the transient polarity defect observed in Gal3-KD cells (38). Alternatively, the polarity defect might result from the suggested role of galectin-3 in apical transport (12). The molecular interactions of galectin-9 are less studied, but its strong affinity to glycolipid-type glycans is of interest (6). Glycolipids play a crucial role in the assembly of basal matrix and can regulate epithelial polarity (40, 41). This aspect warrants further investigating into the role of galectin-9 in epithelial morphogenesis.

Galectins present a significant scientific challenge. They are multivalent and capable of interacting with a number of ligands via various carbohydrate structures. Partially overlapping binding specificities of different galectins further complicate the characterization of their cellular functions. These complex properties probably explain the diverse cellular functions attributed to galectins. It appears that a systematic analysis of the roles of individual galectins in different cell types will be necessary to understand their functions. The combination of RNAi and SCFS allows the study of the contributions by specific proteins to aspects of cell adhesion not assessable with traditional methods. However, it will be important to accumulate more experience with different kinds of samples to better understand the parameters recorded and to realize the full potential of SCFS.

Acknowledgments—We thank Pierre-Henri Puech for invaluable help and advice with SCFS and Clemens Franz for comments on the manuscript. Steffi Dienel and Jaana Träskelin are acknowledged for expert technical assistance.

REFERENCES

- Gibson, M. C., and Perrimon, N. (2003) *Curr. Opin. Cell Biol.* **15**, 747–752
- Mostov, K., Su, T., and ter Beest, M. (2003) *Nat. Cell Biol.* **5**, 287–293
- Nelson, W. J. (2003) *News Physiol. Sci.* **18**, 143–146
- Li, S., Edgar, D., Fassler, R., Wadsworth, W., and Yurchenco, P. D. (2003) *Dev. Cell* **4**, 613–624
- Cooper, D. N. (2002) *Biochim. Biophys. Acta* **1572**, 209–231
- Hirabayashi, J., Hashidate, T., Arata, Y., Nishi, N., Nakamura, T., Hirashima, M., Urashima, T., Oka, T., Futai, M., Muller, W. E. G., Yagi, F., and Kasai, K. (2002) *Biochim. Biophys. Acta* **1572**, 232–254
- Leffler, H., Carlsson, S., Hedlund, M., Qian, Y., and Poirier, F. (2004) *Glycoconj. J.* **19**, 433–440
- Hughes, R. C. (2001) *Biochimie (Paris)* **83**, 667–676
- Bao, Q., and Hughes, R. C. (1995) *J. Cell Sci.* **108**, 2791–2800
- Hikita, C., Vijayakumar, S., Takito, J., Erdjument-Bromage, H., Tempst, P., and Al-Awqati, Q. (2000) *J. Cell Biol.* **151**, 1235–1246
- Delacour, D., Gouyer, V., Zanetta, J. P., Drobecq, H., Leteurtre, E., Grard, G., Moreau-Hannedouche, O., Maes, E., Pons, A., Andre, S., Le Bivic, A., Gabius, H. J., Manninen, A., Simons, K., and Huet, G. (2005) *J. Cell Biol.* **169**, 491–501
- Delacour, D., Cramm-Behrens, C. I., Drobecq, H., Le Bivic, A., Naim, H. Y., and Jacob, R. (2006) *Curr. Biol.* **16**, 408–414
- Poirier, F. (2002) *Biochem. Soc. Symp.* **69**, 95–103
- Maeda, I., Kohara, Y., Yamamoto, M., and Sugimoto, A. (2001) *Curr. Biol.* **11**, 171–176
- Gönczy, P., Echeverri, C., Oegema, K., Coulson, A., Jones, S. J. M., Copley, R. R., Duperon, J., Oegema, J., Brehm, M., Cassin, E., Hannak, E., Kirkham, M., Pichler, S., Flohrs, K., Goessen, A., Leidel, S., Alleaume, A.-M., Martin, C., Özlü, N., Bork, P., and Hyman, A. A. (2000) *Nature* **408**, 331–336
- Meder, D., Shevchenko, A., Simons, K., and Fullekrug, J. (2005) *J. Cell Biol.* **168**, 303–313
- Ojakian, G. K., and Schwimmer, R. (1988) *J. Cell Biol.* **107**, 2377–2387
- Schuck, S., Manninen, A., Honsho, M., Fullekrug, J., and Simons, K. (2004) *Proc. Natl. Acad. Sci. U. S. A.* **101**, 4912–4917
- Matlin, K. S., Haus, B., and Zuk, A. (2003) *Methods* **30**, 235–246
- Aumailley, M., Bruckner-Tuderman, L., Carter, W. G., Deutzmann, R., Edgar, D., Ekblom, P., Engel, J., Engvall, E., Hohenester, E., Jones, J. C. R., Kleinman, H. K., Marinkovich, M. P., Martin, G. R., Mayer, U., Meneguzzi, G., Miner, J. H., Miyazaki, K., Patarroyo, M., Paulsson, M., Quaranta, V., Sanes, J. R., Sasaki, T., Sekiguchi, K., Sorokin, L. M., Talts, J. F., Tryggvason, K., Uitto, J., Virtanen, I., von der Mark, K., Wewer, U. M., Yamada, Y., and Yurchenco, P. D. (2005) *Matrix Biol.* **24**, 326–332
- Hutter, J. L., and Bechhoefer, J. (1993) *Rev. Sci. Instrum.* **64**, 1868–1873
- Jiang, F., Khairy, K., Poole, K., Howard, J., and Muller, D. J. (2004) *Microsc. Res. Tech.* **64**, 435–440
- Grant, D. S., Kleinman, H. K., Leblond, C. P., Inoue, S., Chung, A. E., and Martin, G. R. (1985) *Am. J. Anat.* **174**, 387–398
- Jackson, A. L., Bartz, S. R., Schelter, J., Kobayashi, S. V., Burchard, J., Mao, M., Li, B., Cavet, G., and Linsley, P. S. (2003) *Nat. Biotechnol.* **21**, 635–637
- Puech, P. H., Taubenberger, A., Ulrich, F., Krieg, M., Muller, D. J., and Heisenberg, C. P. (2005) *J. Cell Sci.* **118**, 4199–4206
- Puech, P. H., Poole, K., Knebel, D., and Muller, D. J. (2006) *Ultramicroscopy* **106**, 637–644
- Furtak, V., Hatcher, F., and Ochieng, J. (2001) *Biochem. Biophys. Res. Commun.* **289**, 845–850
- Zegers, M. M., O'Brien, L. E., Yu, W., Datta, A., and Mostov, K. E. (2003) *Trends Cell Biol.* **13**, 169–176
- Taubenberger, A., Cisneros, D. A., Friedrichs, J., Puech, P. H., Muller, D. J., and Franz, C. M. (2007) *Mol. Biol. Cell* **18**, 1634–1644
- Sato, S., Burdett, I., and Hughes, R. C. (1993) *Exp. Cell Res.* **207**, 8–18
- Lindstedt, R., Apodaca, G., Barondes, S. H., Mostov, K. E., and Leffler, H. (1993) *J. Biol. Chem.* **268**, 11750–11757
- Nickel, W. (2005) *Traffic* **6**, 607–614
- Carcamo, C., Pardo, E., Oyanadel, C., Bravo-Zehnder, M., Bull, P., Caceres, M., Martinez, J., Massardo, L., Jacobelli, S., Gonzalez, A., and Soza, A. (2006) *Exp. Cell Res.* **312**, 374–386
- Lagana, A., Goetz, J. G., Cheung, P., Raz, A., Dennis, J. W., and Nabi, I. R. (2006) *Mol. Cell Biol.* **26**, 3181–3193
- Moiseeva, E. P., Williams, B., Goodall, A. H., and Samani, N. J. (2003) *Biochem. Biophys. Res. Commun.* **310**, 1010–1016
- Bao, Q., and Hughes, R. C. (1999) *Glycobiology* **9**, 489–495
- Bullock, S. L., Johnson, T. M., Bao, Q., Hughes, R. C., Winyard, P. J., and Woolf, A. S. (2001) *J. Am. Soc. Nephrol.* **12**, 515–523
- O'Brien, L. E., Jou, T. S., Pollack, A. L., Zhang, Q., Hansen, S. H., Yurchenco, P., and Mostov, K. E. (2001) *Nat. Cell Biol.* **3**, 831–888
- Massa, S. M., Cooper, D. N., Leffler, H., and Barondes, S. H. (1993) *Biochemistry* **32**, 260–267
- Li, S., Liquari, P., McKee, K. K., Harrison, D., Patel, R., Lee, S., and Yurchenco, P. D. (2005) *J. Cell Biol.* **169**, 179–189
- Zinkl, G. M., Zuk, A., van der Bijl, P., van Meer, G., and Matlin, K. S. (1996) *J. Cell Biol.* **133**, 695–708